# Molecular Rectifiers on Silicon: High Performance by Enhancing Top-Electrode/Molecule Coupling

Zachary A. Lamport, <sup>1</sup> Angela D. Broadnax, <sup>2</sup> Ben Scharmann, <sup>1</sup> Robert W. Bradford III, <sup>1</sup> Andrew DelaCourt, <sup>2</sup> Noah Meyer, <sup>1</sup> Hui Li, <sup>2</sup> Scott M. Geyer, <sup>2</sup> Timo Thonhauser, <sup>1</sup> Mark E. Welker, <sup>2</sup> and Oana D. Jurchescu\*, <sup>1</sup>

<sup>1</sup>Department of Physics, Center for Functional Materials, Wake Forest University, Winston-Salem, NC 27109

<sup>2</sup>Department of Chemistry, Center for Functional Materials, Wake Forest University, Winston-Salem, NC 27109

# **KEYWORDS**

molecular electronics, self-assembled monolayer, molecular rectifier, electrode coupling

# **Abstract**

One of the simplest molecular-scale electronic devices is the molecular rectifier. In spite of considerable efforts aimed at understanding structure-property relationships in these systems, however, devices with predictable and stable electronic properties are yet to be developed. Here, we demonstrate highly efficient current rectification in a new class of compounds that form self-assembled monolayers on silicon. We achieve this by exploiting the coupling of the molecules

with the top electrode which, in turn, controls the position of the relevant molecular orbitals. The molecules consist of a silane anchoring group and a nitrogen-substituted benzene ring, separated by a propyl group and imine linkage, and result from a simple, robust, and high-yield synthetic procedure. We find that when incorporated in molecular diodes, these compounds can rectify current by as much as three orders of magnitude, depending on their structure, with a maximum rectification ratio of 2635 being obtained in (E)-1-(4-cyanophenyl)-N-(3-(triethoxysilyl) propyl)methanimine (average  $R_{avg} = 1683 \pm 458$ , at an applied voltage of 2V). This performance is on par with that of the best molecular rectifiers obtained on metallic electrodes, but it has the advantage of lower cost and more efficient integration with current silicon technologies. The development of molecular rectifiers on silicon may yield hybrid systems that can expand the use of silicon towards novel functionalities governed by the molecular species grafted onto its surface.

# Introduction

Electronic devices are ubiquitous to our lives and the quest for ever-smaller and more efficient devices, where commercially available silicon-based technologies have reached their physical limits, has spurred the rise of molecular electronics.  $^{1-12}$  The field of molecular electronics began in 1974 with the pivotal paper by Aviram and Ratner where it was suggested that a single molecule consisting of one electron donor and one acceptor unit connected by a  $\sigma$ -bonded tunneling bridge could rectify current, thus forming a molecular-scale diode which is referred to as the molecular rectifier. This device acts similarly to a solid state diode, allowing the current to flow in one direction and restricting it in the opposite direction. The performance of molecular rectifiers is quantified by the rectification ratio R, which represents the ratio of current density at forward bias compared to the current density at the same magnitude reverse bias. Different strategies were proposed to obtain molecular-scale devices in multilayers, self-assembled monolayers (SAMs),

and a variety of single-molecule techniques. While indeed, current rectification can result from asymmetric Schottky barriers created by the electrodes, in 1993 Martin, et al. showed that the rectification behavior in a donor-acceptor system can originate from the organic layer itself, rather than a work function mismatch between contacts.<sup>14</sup> Although the molecule used in that work differed slightly from the one proposed by Aviram and Ratner, the result was extremely important in showing that the electrical properties of several molecular layers can result in macroscopically significant measurements. Using the same zwitterionic structure, Metzger, et al. proved that rectification is possible not only through multilayered films, but also through an organic monolayer.<sup>15</sup> In 2002, Chabinyc, et al. demonstrated that the donor-acceptor structure is not a prerequisite for current rectification, heralding the introduction of a new class of molecular rectifiers. 16 There have also been many studies on single-molecule charge transport using methods such as mechanically-controlled break junctions, <sup>17–19</sup> scanning tunneling microscopy (STM), <sup>20,21</sup> and conducting probe atomic force microscopy (CP-AFM).<sup>22-25</sup> The field has seen a surge of interest as the fabrication and analysis techniques have become more sophisticated, including the realization of memory circuits based on molecular junctions. 26,27

In spite of the enticing potential of integrating molecular devices with current silicon technologies, most molecular rectifiers adopt thiol-terminated SAMs, which can only bond to metallic substrates. The fabrication of molecular devices on silicon substrates is challenged by the fact that the bond energy associated with the Si-C or Si-O-C covalent bonds formed upon chemisorption of the molecule over the silicon substrate is much larger than that of the metal-S bond characteristic in the case of monolayers on metals, thus limiting the ability of the SAM to migrate between different metal sites. Since the molecular diffusion results in enhanced order, a high degree of order is therefore not easily obtained in molecular layers that bind to

silicon. 6,28 Molecular devices on metals, however, have several disadvantages. First, their adoption in commercial applications would require additional manufacturing steps to allow integration with current technologies. Second, the procedures commonly used for metal deposition (i.e. thermal or electron-beam evaporation) typically yield films with surface roughness that can match or even exceed the lengths of the SAMs, particularly in the case of the short-chained compounds. To circumvent this problem, the template-stripping method was developed wherein metal is deposited onto a silicon wafer and, through the use of a release layer, the metal layer is inverted and transferred to a different substrate.<sup>29,30</sup> While this process has proven effective for fabrication of high performance Au-molecule-metal junctions, its complexity adds significantly to the costs of production of these devices. Transition to silicon substrates could eliminate these issues since silicon is ubiquitous in the current commercial semiconductor industry, making the integration for hybrid devices straightforward. Additionally, the typical roughness of a silicon substrate without any post-processing is lower than 0.1 nm,<sup>31</sup> thus allowing its use without additional steps beyond cleaning. Several studies reported on manufacturing techniques that exploited the thiolate diffusion discussed earlier for self-assembly, followed by integration with silicon. For example, Wheeler's group provided a series of examples where devices have been assembled on the nanometer scale by chemically etching a multilayered silicon-silicon oxide structure and bridging the gap with coated Au nanoparticles. 32,33 Ashwell, et al. used a similar procedure with amino-terminated compounds to form molecular-scale devices which eschewed the metal nanoparticle used in earlier studies, showing that compounds which covalently bond to silicon are viable options.<sup>34,35</sup> Lenfant, et al. gave an example of a sequentially-assembled monolayer on silicon with an e-beam evaporated top contact, but unfortunately the rectification was very modest (maximum rectification ratio of 37 and yield of 50-70%).<sup>36</sup> Hybrid Au-thiol-silicon molecular devices have

been fabricated by using the flip-chip lamination technique, which represented a significant step forward towards the development of silicon-based molecular junctions.<sup>37</sup> These efforts have led to tremendous progress both in manufacturing and understanding basic phenomena occurring in molecular devices, but unfortunately there are still performance criteria to be overcome before adoption in commercial applications. Here, we report on high-performance molecular rectifiers obtained upon the introduction of a strong coupling between the molecules and the top electrode, resulting from the delocalization of the lone pair of electrons from the nitrogen termination to the device electrode. The interaction at the metal/molecule interface alters the position of the molecular orbitals participating in transport, making it efficient for one bias polarity and inefficient for the opposite polarity. The newly developed benzalkylsilane molecules result from a very simple and high-yield synthetic procedure and assemble efficiently on silicon substrates with no need for any pre- or post-processing steps. We obtained a maximum rectification ratio of R = 2635(average  $R_{avg} = 1683 \pm 458$ ), a value that rivals some of the best molecular diodes on metallic surfaces. The ease of synthesis and straightforward assembly on the surface of silicon make these compounds compatible with current electronic devices and may expand the use of silicon technologies towards novel functionalities.

# **Experimental Details**

**Device fabrication.** SAMs comprised of each molecule were constructed on 1 cm  $\times$  1 cm wafers of highly-doped silicon ( $\leq$ 0.005  $\Omega$ cm). The silicon wafers were cleaned first by immersion in hot acetone for 10 minutes followed by a rinse of fresh acetone and isopropyl alcohol (IPA), then a 10-minute immersion in hot IPA, a rinse of fresh IPA and lastly they were dried in a stream of nitrogen. They were then subjected to a 10-minute UV/Ozone treatment, rinsed thoroughly with deionized water, and dried in a stream of nitrogen. The samples were then introduced to a nitrogen

glovebox (<0.1 ppm H2O, <0.1 ppm O2) and submerged in a 4 mMol solution of one of Compounds 1-7 in chloroform for 18-24 hours. Following the SAM deposition, the samples were removed from the glovebox, rinsed thoroughly with fresh chloroform and IPA, and dried in a stream of nitrogen, then measured immediately. Contact angle measurements were used to characterize the order within the SAM and to determine the best method for its deposition, the results are displayed in Figure S1 and Table S1, Supporting Information.

Electrical characterization. The molecular rectifiers were characterized using an EGaIn (Eutectic gallium-indium) probe tip as the top electrode. The probe was constructed by depositing a small amount of EGaIn onto a sacrificial copper strip into which a 0.5 mm diameter tungsten probe was lowered and then gently raised using a Micromanipulator. The silicon substrate was grounded and the potential was applied at the top electrode in an ambient probe station. At least 200 measurements resulting from a minimum of 5 samples were collected for each type of SAM to allow for an accurate statistical analysis.

Cyclic Voltammetry. In order to determine the position of the highest occupied molecular orbital (HOMO), cyclic voltammetry measurements were carried out using 0.1 M tetrabutylammonium tetrafluoroborate in acetonitrile, a Pt counter-electrode, and an Ag/AgCl reference. The system was calibrated using the Fc/Fc+ redox potential (0.6 V vs. Ag). The scans were taken at a scan rate of 20 mV/s using the silicon wafer treated with the SAM under examination as the working electrode.

**Theory.** Our *ab initio* calculations have been performed at the density functional theory (DFT) level, as implemented in VASP.<sup>38</sup> We employed the standard projector augmented wave (PAW) potentials that are provided with the package together with the PBE exchange-correlation functional.<sup>39</sup> We also checked more advanced hybrid functionals such as HS03,<sup>40</sup> HS06,<sup>41</sup> and

B3LYP,<sup>42</sup> which can provide an improved description of excited states.<sup>43</sup> However, we found that their calculated band gaps all were within 3% of the PBE gap (this is somewhat unexpected, as simple GGA functionals like PBE are typically not highly accurate in describing the band gap). A plane-wave kinetic energy cutoff of 600 eV and an energy convergence criterion of  $1x10^{-4}$  eV were used. We simulated the gas-phase of the various molecules by putting them in boxes of appropriate sizes, ensuring that we had at least 10 Å of vacuum between periodic replica to eliminate spurious interactions; only the  $\Gamma$ -point was sampled. All molecules were relaxed until the forces on each atom were smaller than 1 meV/Å. The vacuum level was calculated by evaluating the potential away from the molecule at a point where it becomes constant.

# Results and Discussion

The model system that we introduce is (E)-1-(4-cyanophenyl)-N-(3-(triethoxysilyl) propyl)methanimine (CPh-TPI - Compound 1, chemical structure is shown in Figure 1a). The molecule consists of two asymmetric anchoring moieties and a decoupling bridge between them: the triethoxysilane ensures chemisorption to the bottom silicon electrode and the nitrile ( $-C\equiv N$ ) physisorbs on the top EGaIn electrode. The lone pair of the N-atom will interact with the  $Ga_2O_3$  layer that coats the electrode surface. <sup>44</sup> Gallium oxide is known to be a strong Lewis acid capable of tight binding to linear *sp* hybridized organic molecules/moieties such as CO or -CN functional group. <sup>45</sup> This Lewis-acid-Lewis base interaction can therefore occur through N in this case, providing a well-defined electronic coupling between the SAM and the top electrode, which is key to the enhanced rectification. The alkyl chain inhibits the  $\pi$ -coupling between the two end fragments to a certain extent, while the  $\pi$ - $\pi$  interactions between neighboring phenyl groups enhances the order of the SAM on the substrate. <sup>46</sup> Details on the synthesis are included in the Supporting Information. Figure 1b shows the molecular rectifier structure, where the bottom

electrode was highly-doped silicon with a native layer of silicon oxide upon which a SAM of this compound was assembled, and the top electrode was a cone of the liquid metal EGaIn. A bias was applied to the EGaIn electrode with the silicon electrode held at ground, and the current was measured at forward and reverse bias, of up to +2 V and -2 V.

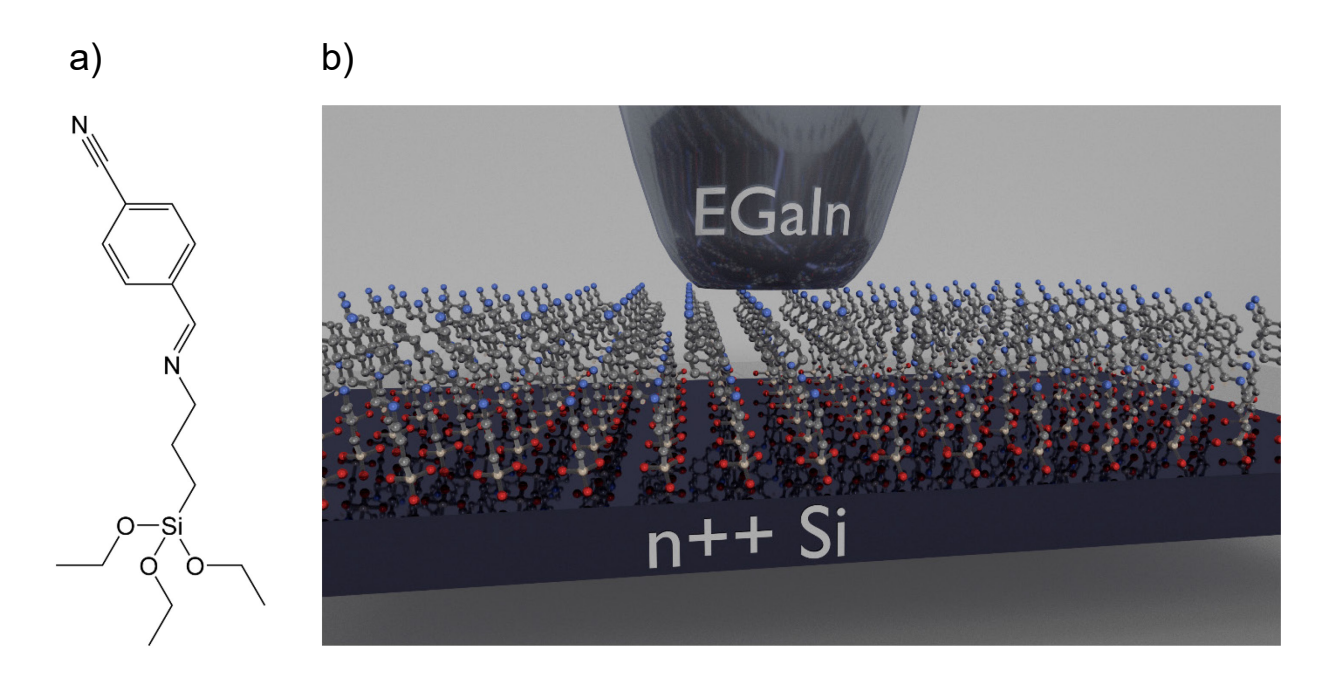


**Figure 1.** (a) Chemical structure of CPh-TPI, (b) Device structure of the molecular rectifiers showing the liquid metal EGaIn probe tip, the SAM under test, and the highly-doped silicon substrate. The preferred direction of electron flow is from the Si substrate to the EGaIn top electrode.

In Figures 2a and 2b we show the average current density (J) as a function of applied voltage (V) through our SAM on both a linear and a logarithmic scale. It can be observed that charge transport is more efficient in the forward bias regime, similar to the case of a solid-state diode. The average current density curve shown in Figure 2 was obtained by taking the average current density from 100 J-V curves obtained on different samples (multiple spots on one sample, as well as

several SAM films). The small standard deviation in current density indicates good uniformity in the electrical properties of the films, which is of paramount importance in any new technology. The rectification ratio, R, was calculated as the ratio of current density at forward bias compared to the current density at negative bias:

$$R = \frac{J(V_{fwd} = +2V)}{J(V_{rev} = -2V)} \tag{1}$$

where the current density is obtained by dividing the measured current by the area of the EGaIn probe tip. The results are summarized in the histogram presented in Figure 2c. In the inset of this figure, the average and maximum rectification ratio obtained are listed. The highest rectification strength was  $R_{max} = 2635$  with an average of  $R_{avg} = 1683 \pm 458$ . To the best of our knowledge, this value represents the highest rectification ratio obtained from a SAM on silicon. We note that higher rectification ratios have been attained using thiolated SAMs on Ag;<sup>47</sup> however these results were obtained at higher voltages, and the devices require complex fabrication procedures to produce the ultra-smooth substrates necessary for molecular electronics. Conversely, fabrication of molecular

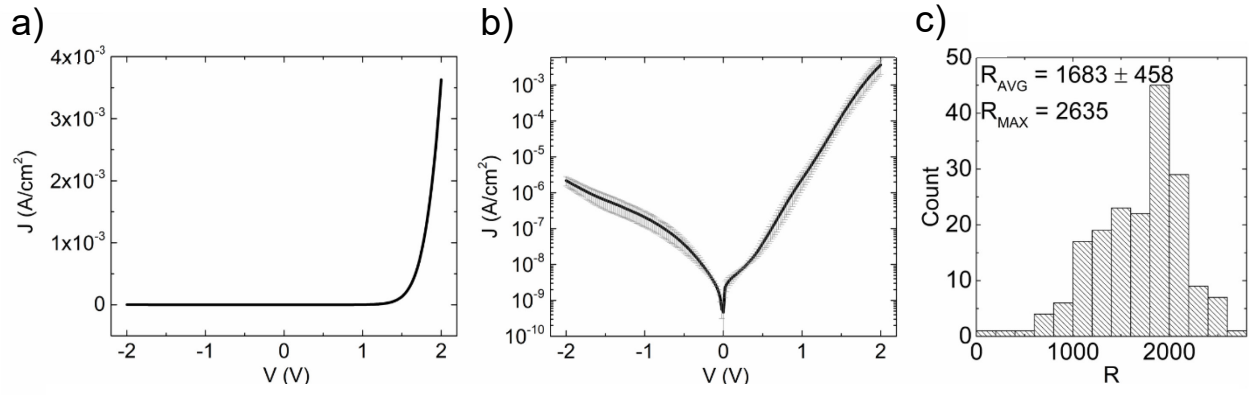


**Figure 2.** (a) The average J-V curve for CPh-TPI (Compound 1) on a linear scale, showing the diode-like rectification. (b) The average J-V curve for CPh-TPI on a logarithmic scale where the scale bars show the standard deviation. (c) A histogram of rectification ratios for CPh-TPI. The maximum and average rectification values are included in the inset.

rectifiers using silanes deposited on silicon does not require significant processing to ensure the formation of robust monolayers. In addition to the high performance shown in devices, these compounds are synthetically simple to make, utilizing condensation chemistry. The rectification behavior seems to be very stable to bias stress, as suggested by the successive measurements taken on the same spot (without moving the EGaIn probe tip); the results are displayed in Figure S2.

To confirm our hypothesis that the N lone pair is responsible for the enhanced rectification, we designed and tested several different types of molecules whose end-substituents allow for tuning the molecule/top electrode coupling at the interface with EGaIn, while keeping the interaction at the silicon interface constant. The chemical structures of these compounds with their rectification 2 ratios displayed Figure 3. Compound ((E)-1-phenyl-N-(3are in (triethoxysilyl)propyl)methanimine) is identical to CPh-TPI except that it is missing the -CN terminal group that facilitates the interaction with the top electrode. With this interaction being absent, we found that the current rectification is less efficient, with an average rectification being almost one order of magnitude lower than in the case of CPh-TPI,  $R_{avg} = 221 \pm 177$ . Most likely, the different structure of this molecule will also yield differences in the energy-level alignment of the highest occupied molecular orbital/lowest unoccupied molecular orbital (HOMO/LUMO) levels relative to the metal Fermi energy, as well as the SAM degree of order on the substrate, both factors that influence the rectification behavior. Nevertheless, the significant reduction in rectification is clear and we argue that the lack of molecule/ top electrode coupling is the main origin of the inefficient current rectification found in devices of Compound 2. Another example is Compound 3 ((E)-1-(4-nitrophenyl)-N-(3-(triethoxysilyl)propyl)methanimine). In this case, the N atom is  $sp^2$  hybridized, and therefore has no lone pair that would facilitate coupling with the top electrode. As a result, the rectification ratio is also low,  $R_{avg} = 202\pm92$ . In Compound 4 ((E)-1-(4-

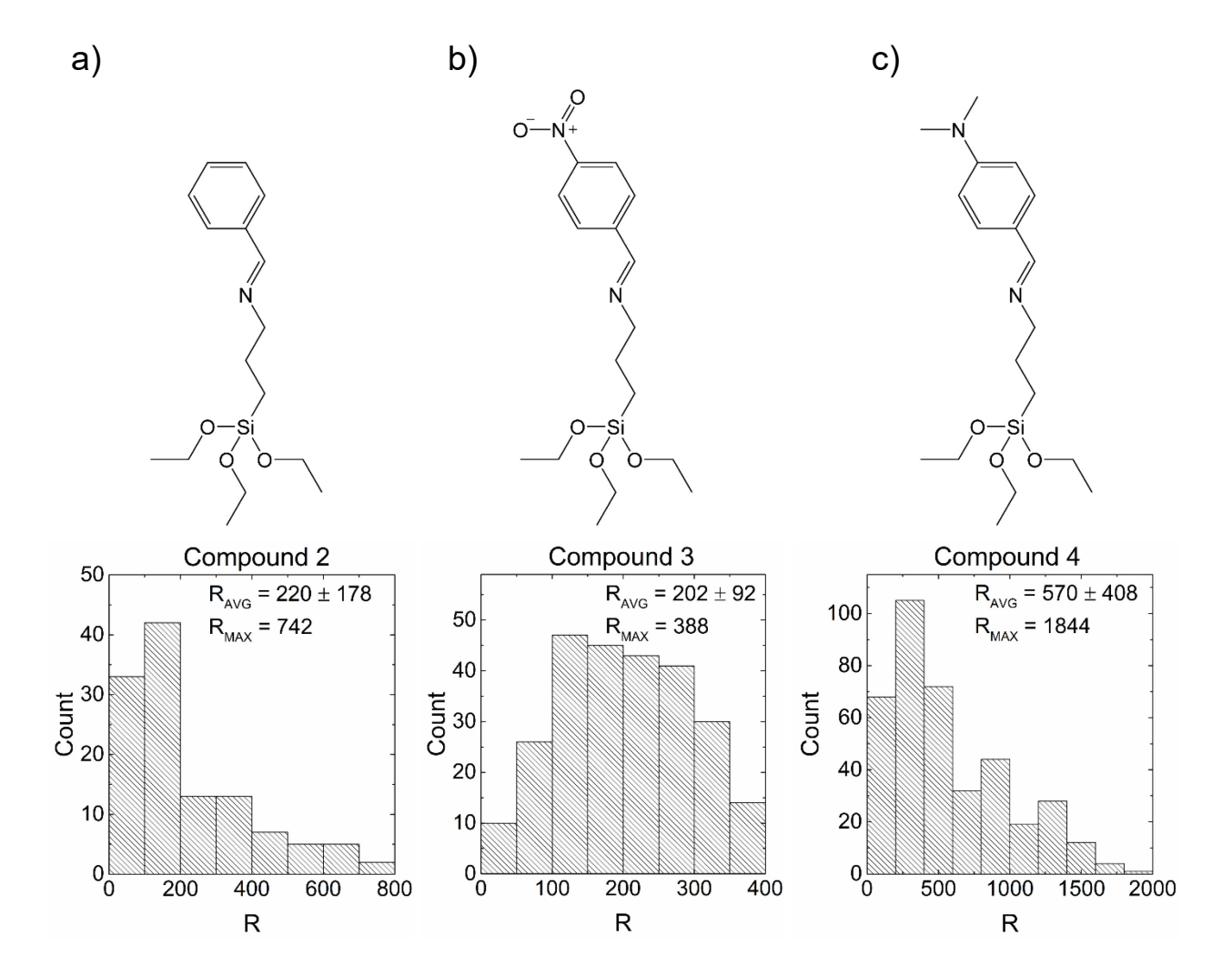


**Figure 3.** Chemical structure and histogram of rectification ratios for (a) Compound 2, (b) Compound 3, and (c) Compound 4. For all molecules the preferred direction of electron flow is from the Si substrate to the EGaIn top electrode.

N,N-dimethylaminophenyl)-N-(3-(triethoxysilyl)propyl)methanimine), N is  $sp^3$  hybridized, so the lone pair is present. As expected, the rectification,  $R_{avg} = 569 \pm 408$ , is larger than in Compounds 2 or 3, but as access to the non-bonding pair of electrons is attenuated due to the steric hindrance introduced by the bulky  $-CH_3$  substituents, it remains inferior to CPh-TPI. To explore the validity of our hypothesis even further, we investigated the properties of molecules containing two benzene

rings in the bridge between the two anchoring groups. Compounds 5 ((E)-4'-(((3-(triethoxysilyl)propyl)imino)methyl)-[1,1'-biphenyl]-4-carbonitrile) and ((E)-1-([1,1]'biphenyl]-4-yl)-N-(3-(triethoxysilyl)propyl)methanimine), shown in Figure S3a and b, differ only in the end-substituent. Similar to the case of CPh-TPI and Compound 2, the presence of -CN leads to a higher rectification ratio:  $R_{avg} = 700\pm347$  for Compound 5 and  $R_{avg} = 215\pm176$  for Compound 6. The variability in the properties of these compounds is by no means a linear relationship, as not only does the rectification depend on the relative molecular orbital's energetic position and the physical asymmetry of each molecule, but also the local electric field, the molecular disorder, and the molecular density. Compound 5, for example, showed a maximum rectification of  $R_{max} = 2413$ in a system similar to that of CPh-TPI, but with an extended  $\pi$ -structure. The lower value measured in SAMs of Compound 5 can be understood in the context of molecular asymmetry, since the  $\pi$ structure extends over a larger proportion of Compound 5. The difference between bias at one polarity and bias at the opposing polarity is therefore smaller than that in CPh-TPI. We also examined the role of the nitrogen termination in SAMs containing an alkyl-chain only in the decoupling unit and no benzene ring. Compound 7 (Figure S3c) exhibits a maximum rectification ratio of  $R_{max} = 882$  and an average of  $R_{avg} = 356 \pm 164$ . This result indicates that SAMs of nitrogenterminated compounds with non-bonding electrons can efficiently rectify current even in the absence of the  $\pi$ -conjugation when a partial charge transfer to the EGaIn electrode occurs.

The examples included above provide conclusive evidence that the N lone pair can control the transport mechanism in a molecular rectifier when its interaction with the electrode surface is allowed. Note that the molecule/top-electrode interaction via the N lone pair is fundamentally different than the one proposed in the case ferrocenyl/Ag coupling.<sup>48</sup> Next, we will propose a mechanism through which the metal–molecule coupling impacts the electronic transport through

the rectifier and therefore the rectification. The pre-requisite for current rectification is the presence of an asymmetry within the device. This can be located within the molecular structure and/or device architecture (asymmetric Schottky barriers).<sup>49,50</sup> To elucidate the contribution of the difference in work functions of the silicon and EGaIn electrodes to current rectification, we evaluated a blank sample in which the EGaIn was in direct contact with the silicon wafer; the resulting *J-V* curve is shown in Figure S4. The work functions of the EGaIn and silicon electrodes are -4.2 eV and -4.65 eV, respectively, raising the possibility of a Schottky mechanism when comparing forward to reverse bias.<sup>31,44</sup> However, as the electrical characteristics in Figure S4 show, there is negligible current rectification in this sample, and therefore the observed rectification is solely the result of the presence of the molecule.

To understand what factors determine the properties of our high-performance molecular rectifiers, we started by analyzing the electronic properties of an isolated molecule of Compound

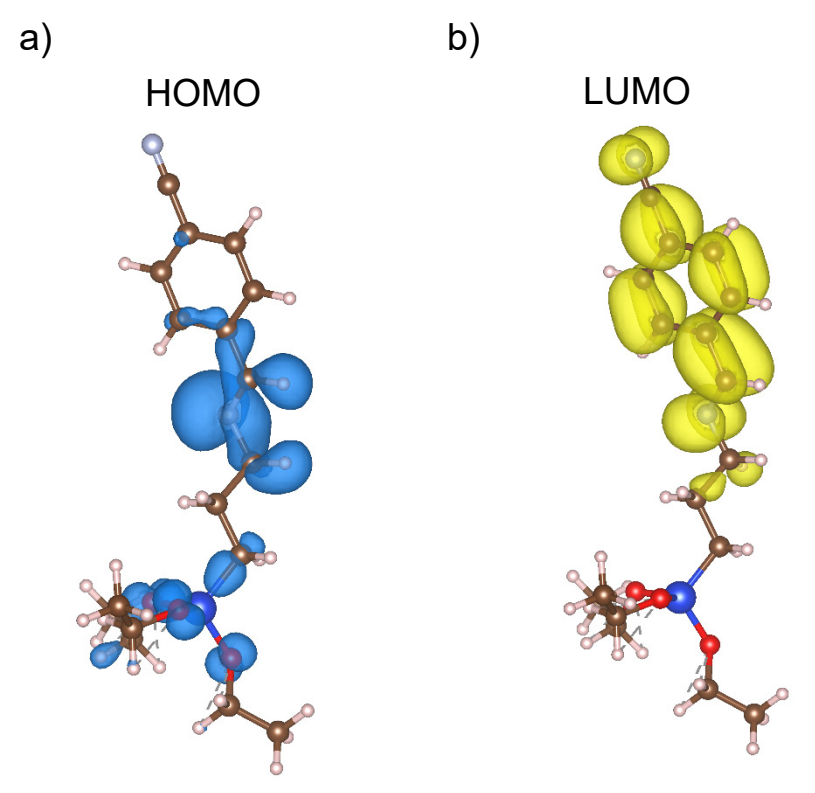


**Figure 4.** (a) HOMO and (b) LUMO of Compound 1 depicted as their corresponding band-decomposed charge densities, plotted at an iso-level of  $1.5 \times 10^{-3} \ e/\text{Å}^3$ .

1 via *ab initio* simulations at the DFT level—for details about our calculations, see the Methods section. The calculated values for the HOMO and LUMO of Compound 1 (referenced to the vacuum level) are -6.28 eV and -3.16 eV respectively, giving an energy gap of 3.12 eV. This result is in excellent agreement with the cyclic voltammetry measurements shown in Figure S5, where we found a value of -6.3 eV for the HOMO level. The results for all compounds are summarized in Table S2 in the supplementary information and we find little correlation between the HOMO/LUMO position or the value of the gap and the rectification ratio. However, it is known that when the coupling between the molecule and electrode is strong, the positions of the HOMO and LUMO levels in the device are different from those of the isolated molecule since the

interaction at the molecule/electrode interface governs the energetic picture. 51,52 It is therefore not surprising that no correlations were observed for the insulated molecules and the measured rectification behavior. In Figure 4 we show the corresponding HOMO and LUMO states in terms of their band-decomposed charge densities for Compound 1 (results for all molecules are provided in Figures S6-S11, Supplementary Information). We find that the HOMO is extended along the silane anchoring group and the alkyl chain, while the LUMO is localized on the ring and the nitrile end group. The part of the LUMO on the very top (i.e. the nitrile group) facilitates electron transfer from the EGaIn in contact with the molecule. When the isolated molecules are then assembled in a monolayer, which is the case in our devices, the intermolecular interactions modify the energy landscape, typically yielding a compression of the gap. 51,53,54 In addition, the coupling with the electrodes results in further compression arising from a pinning effect at the molecule/contact interfaces. 51,53,55 The corresponding band diagram of the SAM sandwiched between the silicon and EGaIn electrodes at zero applied bias is proposed in Figure 5a where LUMO\* and HOMO\* indicate the altered frontier orbitals when in contact with the two metals, and  $\Delta \varphi$  represents the energy difference between the Fermi energies of the top and bottom electrodes. When a positive voltage is applied between the top EGaIn electrode and the grounded silicon bottom electrode, the strong coupling between the nitrile group and Ga<sub>2</sub>O<sub>3</sub> causes a Fermi level pinning, similar to the case of nitrile/Au.<sup>51</sup> As a result, the LUMO\* of the molecule follows the Fermi level of this electrode, a feature that dominates the transport and leads to further compression of the bandgap as the voltage increases. This phenomenon promotes the placement of the LUMO\* in the transmission window, allowing for resonant tunneling, an efficient charge transport mechanism that leads to high conductivity (Figure 5b). On the contrary, when a negative voltage is applied, the Fermi level pinning effect results in a shift such that the LUMO\* is no longer in the

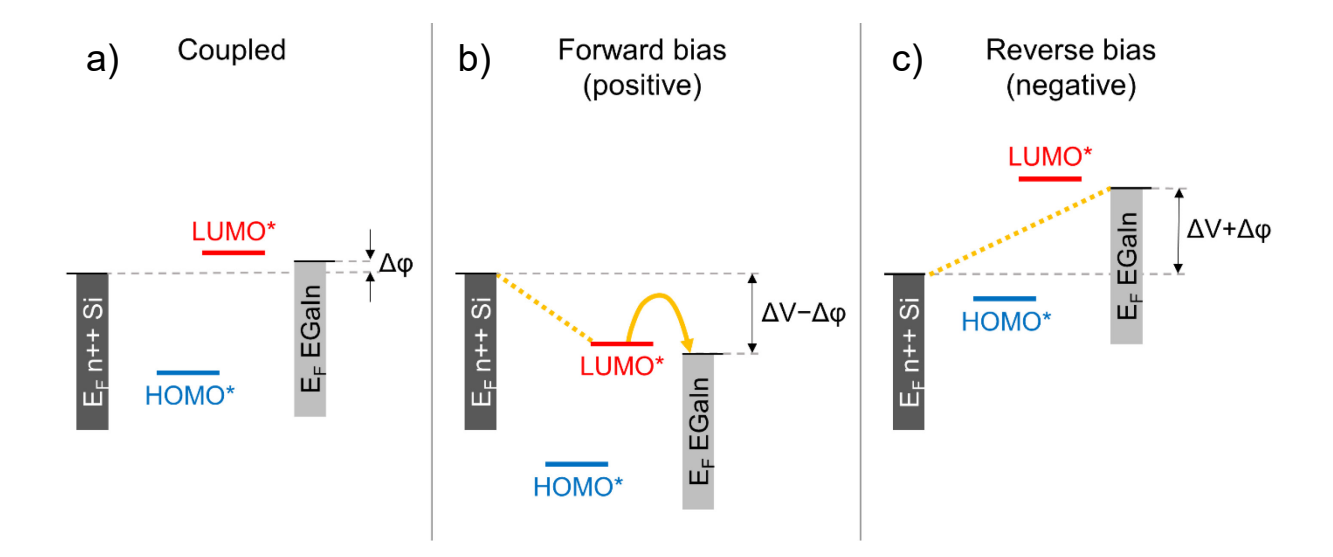


**Figure 5.** (a) The energetic landscape of the test compounds showing the frontier orbitals under the influence of the electrodes, HOMO\* and LUMO\*, with  $\Delta \varphi$  being the energy difference between silicon and the EGaIn electrode, (b) The same energetic landscape with a positive bias  $\Delta V$  applied to the EGaIn electrode, and (c) with a negative bias  $\Delta V$  applied to the EGaIn electrode. The dashed yellow line indicates nonresonant tunneling while the solid yellow line represents resonant tunneling.

transmission window. In this case, the transport can only occur via nonresonant tunneling, which is the origin of low conductivity across the junction (Figure 5c). These phenomena, in which the molecular orbital participates in transport under one polarity of the bias, but not under the other one, as depicted in Figures 5b and 5c, collectively produce a high rectification. When the molecule is strongly coupled to the electrode, such as the case of Compounds 1 and 5, this interfacial interaction gives rise to a Fermi level pinning. In this case, the position of the relevant molecular orbitals in the junction is controlled by the potential applied at the electrodes, with only minimal contributions from the intrinsic properties of the SAM, resulting in bandgap compression and a

transition between two different charge transport mechanisms upon sweeping the voltage. The consequence is the ability of these devices to rectify the current very efficiently. When the coupling is weak or absent, only the molecular asymmetries are the origin of rectification, such as is the case of Compounds 2, 3, 4, and 6 from this study, as well as the fluorinated benzalkylsilanes and ferrocenealkylsilanes reported by us in the past. These devices are limited to rectifications on the order of 100. In the proposed rectification mechanism we ignored the presence of the Ga<sub>2</sub>O<sub>3</sub> layer between the SAM and the EGaIn electrode: this assumption is validated by experimental results that demonstrated the Ga<sub>2</sub>O<sub>3</sub> layer does not contribute to rectification.

# Conclusions

In summary, we showed that highly efficient molecular rectifiers can be obtained in SAMs containing terminal groups that promote a strong coupling with the electrodes, which leads to Fermi level pinning. This effect controls the position of the relevant molecular orbitals and modulates the energy gap. Our rectifiers take advantage of the spontaneous assembly of the molecular layer on a silicon substrate via chemisorption, a process that is both simple and efficient. The SAMs originate from a simple and high-yield synthetic procedure, a key attribute for low-cost electronics. The highest rectification ratio exceeds 2000, a value that rivals the highest performance rectifiers obtained on metallic substrates, but with the added advantage of a straightforward integration with current technologies.

### ASSOCIATED CONTENT

# **Supporting Information.**

Additional results including water droplet contact angle data, bias stress stability of Compound

1, rectification data for Compounds 5-7, J-V characteristics on clean native silicon oxide, cyclic

voltammetry, HOMO and LUMO states in terms of the band-decomposed charge densities,

synthesis of Compounds 1-6, and spectral analysis.

**AUTHOR INFORMATION** 

**Corresponding Author** 

\*E-mail: jurchescu@wfu.edu

**Author Contributions** 

The manuscript was written through contributions of all authors. All authors have given approval

to the final version of the manuscript.

ACKNOWLEDGMENT

This work was partially supported by the National Science Foundation under grant ECCS

1254757.

REFERENCES

**(1)** Nijhuis, C. A.; Reus, W. F.; Barber, J. R.; Dickey, M. D.; Whitesides, G. M. Charge

Transport and Rectification in Arrays of SAM-Based Tunneling Junctions. *Nano Lett.* **2010**,

*10*, 3611–3619.

(2) Metzger, R. M. Unimolecular Electronics. Chem. Rev. 2015, 115, 5056–5115.

(3) Reus, W. F.; Thuo, M. M.; Shapiro, N. D.; Nijhuis, C. A.; Whitesides, G. M. The SAM, Not

the Electrodes, Dominates Charge Transport in Metal-Monolayer//Ga 2 O 3 /Gallium-

18

- Indium Eutectic Junctions. ACS Nano 2012, 6, 4806–4822.
- (4) Song, P.; Guerin, S.; Tan, S. J. R.; Annadata, H. V.; Yu, X.; Scully, M.; Han, Y. M.; Roemer, M.; Loh, K. P.; Thompson, D.; Nijhuis, C. A. Stable Molecular Diodes Based on π-π Interactions of the Molecular Frontier Orbitals with Graphene Electrodes. *Adv. Mater.* 2018, 30, 1706322.
- (5) Metzger, R. M. Quo Vadis, Unimolecular Electronics? *Nanoscale* **2018**, *10*, 10316–10332.
- (6) Vilan, A.; Yaffe, O.; Biller, A.; Salomon, A.; Kahn, A.; Cahen, D. Molecules on Si: Electronics with Chemistry. *Adv. Mater.* **2010**, *22*, 140–159.
- (7) Vilan, A.; Aswal, D.; Cahen, D. Large-Area, Ensemble Molecular Electronics: Motivation and Challenges. *Chem. Rev.* **2017**, *117*, 4248–4286.
- (8) McCreery, R. L.; Yan, H.; Bergren, A. J. A Critical Perspective on Molecular Electronic Junctions: There Is Plenty of Room in the Middle. *Phys. Chem. Chem. Phys.* 2013, 15, 1065–1081.
- (9) Yuan, L.; Breuer, R.; Jiang, L.; Schmittel, M.; Nijhuis, C. A. A Molecular Diode with a Statistically Robust Rectification Ratio of Three Orders of Magnitude. *Nano Lett.* **2015**, *15*, 5506–5512.
- (10) Jeong, H.; Kim, D.; Xiang, D.; Lee, T. High-Yield Functional Molecular Electronic Devices. *ACS Nano* **2017**, *11*, 6511–6548.
- (11) Xiang, D.; Wang, X.; Jia, C.; Lee, T.; Guo, X. Molecular-Scale Electronics: From Concept to Function. *Chem. Rev.* **2016**, *116*, 4318–4440.
- (12) Yuan, L.; Nerngchamnong, N.; Cao, L.; Hamoudi, H.; del Barco, E.; Roemer, M.; Sriramula, R. K.; Thompson, D.; Nijhuis, C. A. Controlling the Direction of Rectification in a Molecular Diode. *Nat. Commun.* **2015**, *6*, 6324.

- (13) Aviram, A.; Ratner, M. A. Molecular Rectifiers. Chem. Phys. Lett. 1974, 29, 277.
- (14) Martin, A. S.; Sambles, J. R.; Ashwell, G. J. Molecular Rectifier. *Phys. Rev. Lett.* **1993**, 70, 218–221.
- (15) Metzger, R. M.; Chen, B.; Höpfner, U.; Lakshmikantham, M. V.; Vuillaume, D.; Kawai, T.; Wu, X.; Tachibana, H.; Hughes, T. V.; Sakurai, H.; Baldwin, J. W.; Hosch, C.; Cava, M. P.; Brehmer, L.; Ashwell, G. J. Unimolecular Electrical Rectification in Hexadecylquinolinium Tricyanoquinodimethanide. J. Am. Chem. Soc. 1997, 119, 10455–10466.
- (16) Chabinyc, M. L.; Chen, X.; Holmlin, R. E.; Jacobs, H.; Skulason, H.; Frisbie, C. D.; Mujica, V.; Ratner, M. A.; Rampi, M. A.; Whitesides, G. M. Molecular Rectification in a Metal-Insulator-Metal Junction Based on Self-Assembled Monolayers. *J. Am. Chem. Soc.* 2002, 124, 11730–11736.
- (17) Reed, M. A.; Zhou, C.; Muller, C. J.; Burgin, T. P.; Tour, J. M. Conductance of a Molecular Junction. *Science* (80-. ). **1997**, 278, 252–254.
- (18) Batra, A.; Darancet, P.; Chen, Q.; Meisner, J. S.; Widawsky, J. R.; Neaton, J. B.; Nuckolls,
  C.; Venkataraman, L. Tuning Rectification in Single-Molecular Diodes. *Nano Lett.* 2013,
  13, 6233–6237.
- (19) Perrin, M. L.; Galán, E.; Eelkema, R.; Thijssen, J. M.; Grozema, F.; van der Zant, H. S. J. A Gate-Tunable Single-Molecule Diode. *Nanoscale* **2016**, *8*, 8919–8923.
- (20) Xu, B.; Tao, N. J. Measurement of Single-Molecule Resistance by Repeated Formation of Molecular Junctions. *Science* (80-. ). **2003**, 301, 1221–1223.
- (21) Joachim, C.; Gimzewski, J. K.; Schlittler, R. R.; Chavy, C. Electronic Transparence of a Single C60 Molecule. *Phys. Rev. Lett.* **1995**, *74*, 2102–2105.

- (22) Wold, D. J.; Frisbie, C. D. Formation of Metal-Molecule-Metal Tunnel Junctions: Microcontacts to Alkanethiol Monolayers with a Conducting AFM Tip. J. Am. Chem. Soc. 2000, 122, 2970–2971.
- (23) Wold, D. J.; Frisbie, C. D. Fabrication and Characterization of Metal–Molecule–Metal Junctions by Conducting Probe Atomic Force Microscopy. *J. Am. Chem. Soc.* **2001**, *123*, 5549–5556.
- (24) Kim; Beebe, J. M.; Jun, Y.; Zhu, X.-Y.; Frisbie, C. D. Correlation between HOMO Alignment and Contact Resistance in Molecular Junctions: Aromatic Thiols versus Aromatic Isocyanides. *J. Am. Chem. Soc.* **2006**, *128*, 4970–4971.
- (25) Ho Choi, S.; Kim, B.; Frisbie, C. D. Electrical Resistance of Long Conjugated Molecular Wires. *Science* (80-. ). **2008**, 320, 1482–1486.
- (26) Green, J. E.; Choi, J. W.; Boukai, A.; Bunimovich, Y.; Johnston-Halperin, E.; DeIonno, E.; Luo, Y.; Sheriff, B. A.; Xu, K.; Shin, Y. S.; Tseng, H.-R.; Stoddart, J. F.; Heath, J. R. A 160-Kilobit Molecular Electronic Memory Patterned at 10(11) Bits per Square Centimetre. Nature 2007, 445, 414–417.
- (27) Reed, M. A.; Chen, J.; Rawlett, A. M.; Price, D. W.; Tour, J. M. Molecular Random Access Memory Cell. *Appl. Phys. Lett.* **2001**, *78*, 3735–3737.
- (28) Ulman, A. Formation and Structure of Self-Assembled Monolayers. *Chem. Rev.* **1996**, *96*, 1533–1554.
- (29) Hegner, M.; Wagner, P.; Semenza, G. Ultralarge Atomically Flat Template-Stripped Au Surfaces for Scanning Probe Microscopy. *Surf. Sci.* **1993**, *291*, 39–46.
- (30) Weiss, E. A.; Kaufman, G. K.; Kriebel, J. K.; Li, Z.; Schalek, R.; Whitesides, G. M. Si/SiO 2 -Templated Formation of Ultraflat Metal Surfaces on Glass, Polymer, and Solder

- Supports: Their Use as Substrates for Self-Assembled Monolayers. *Langmuir* **2007**, *23*, 9686–9694.
- Lamport, Z. A.; Broadnax, A. D.; Harrison, D.; Barth, K. J.; Mendenhall, L.; Hamilton, C.
  T.; Guthold, M.; Thonhauser, T.; Welker, M. E.; Jurchescu, O. D. Fluorinated
  Benzalkylsilane Molecular Rectifiers. Sci. Rep. 2016, 6, 38092.
- (32) Dirk, S. M.; Howell, S. W.; Zmuda, S.; Childs, K.; Blain, M.; Simonson, R. J.; Wheeler, D. R. Novel One-Dimensional Nanogap Created with Standard Optical Lithography and Evaporation Procedures. *Nanotechnology* 2005, 16, 1983–1985.
- (33) Howell, S. W.; Dirk, S. M.; Childs, K.; Pang, H.; Blain, M.; Simonson, R. J.; Tour, J. M.; Wheeler, D. R. Mass-Fabricated One-Dimensional Silicon Nanogaps for Hybrid Organic/Nanoparticle Arrays. *Nanotechnology* **2005**, *16*, 754–758.
- (34) Ashwell, G. J.; Phillips, L. J.; Robinson, B. J.; Urasinska-Wojcik, B.; Lambert, C. J.; Grace, I. M.; Bryce, M. R.; Jitchati, R.; Tavasli, M.; Cox, T. I.; Sage, I. C.; Tuffin, R. P.; Ray, S. Molecular Bridging of Silicon Nanogaps. ACS Nano 2010, 4, 7401–7406.
- (35) Ashwell, G. J.; Phillips, L. J.; Robinson, B. J.; Barnes, S. A.; Williams, A. T.; Urasinska-Wojcik, B.; Lambert, C. J.; Grace, I. M.; Cox, T. I.; Sage, I. C. Synthesis of Covalently Linked Molecular Bridges between Silicon Electrodes in CMOS-Based Arrays of Vertical Si/SiO 2/Si Nanogaps. *Angew. Chemie Int. Ed.* 2011, 50, 8722–8726.
- (36) Lenfant, S.; Krzeminski, C.; Delerue, C.; Allan, G.; Vuillaume, D. Molecular Rectifying Diodes from Self-Assembly on Silicon. *Nano Lett.* **2003**, *3*, 741–746.
- (37) Coll, M.; Miller, L. H.; Richter, L. J.; Hines, D. R.; Jurchescu, O. D.; Gergel-Hackett, N.; Richter, C. A.; Hacker, C. A. Formation of Silicon-Based Molecular Electronic Structures Using Flip-Chip Lamination. *J. Am. Chem. Soc.* **2009**, *131*, 12451–12457.

- (38) Kresse, G.; Furthmüller, J. Efficient Iterative Schemes for Ab Initio Total-Energy Calculations Using a Plane-Wave Basis Set. *Phys. Rev. B* **1996**, *54*, 11169–11186.
- (39) Perdew, J. P.; Burke, K.; Ernzerhof, M. Generalized Gradient Approximation Made Simple. *Phys. Rev. Lett.* **1996**, *77*, 3865–3868.
- (40) Heyd, J.; Scuseria, G. E.; Ernzerhof, M. Hybrid Functionals Based on a Screened Coulomb Potential. *J. Chem. Phys.* **2003**, *118*, 8207–8215.
- (41) Heyd, J.; Scuseria, G. E.; Ernzerhof, M. Erratum: "Hybrid Functionals Based on a Screened Coulomb Potential" [J. Chem. Phys. 118, 8207 (2003)]. *J. Chem. Phys.* 2006, 124, 219906.
- (42) Stephens, P. J.; Devlin, F. J.; Chabalowski, C. F.; Frisch, M. J. Ab Initio Calculation of Vibrational Absorption and Circular Dichroism Spectra Using Density Functional Force Fields. J. Phys. Chem. 1994, 98, 11623–11627.
- (43) Garza, A. J.; Scuseria, G. E. Predicting Band Gaps with Hybrid Density Functionals. *J. Phys. Chem. Lett.* **2016**, *7*, 4165–4170.
- (44) Chiechi, R. C.; Weiss, E. A.; Dickey, M. D.; Whitesides, G. M. Eutectic Gallium-Indium (EGaIn): A Moldable Liquid Metal for Electrical Characterization of Self-Assembled Monolayers. *Angew. Chemie Int. Ed.* 2008, 47, 142–144.
- (45) Rodríguez Delgado, M.; Morterra, C.; Cerrato, G.; Magnacca, G.; Otero Areán, C. Surface Characterization of γ-Ga 2 O 3 : A Microcalorimetric and IR Spectroscopic Study of CO Adsorption. *Langmuir* 2002, 18, 10255–10260.
- (46) Dou, R.-F.; Ma, X.-C.; Xi, L.; Yip, H. L.; Wong, K. Y.; Lau, W. M.; Jia, J.-F.; Xue, Q.-K.; Yang, W.-S.; Ma, H.; Jen, A. K.-Y. Self-Assembled Monolayers of Aromatic Thiols Stabilized by Parallel-Displaced Π-π Stacking Interactions. *Langmuir* 2006, 22, 3049–3056.

- (47) Chen, X.; Roemer, M.; Yuan, L.; Du, W.; Thompson, D.; del Barco, E.; Nijhuis, C. A. Molecular Diodes with Rectification Ratios Exceeding 105 Driven by Electrostatic Interactions. *Nat. Nanotechnol.* 2017, 12, 797–803.
- (48) Wei, M.-Z.; Yu, X.; Fu, X.-X.; Wang, Z.-Q.; Wang, C.-K.; Zhang, G.-P. Controlling Rectification Performance by Tuning Molecule–Electrode Coupling Strength in Ferrocenyl-Undecanethiolate Molecular Diodes. *J. Phys. Chem. C* **2019**, *123*, 1559–1565.
- (49) Kornilovitch, P. E.; Bratkovsky, A. M.; Williams, R. S. Current Rectification by Molecules with Asymmetric Tunneling Barriers. *Phys. Rev. B* **2002**, *66*, 165436.
- (50) Pan, J. B.; Zhang, Z. H.; Ding, K. H.; Deng, X. Q.; Guo, C. Current Rectification Induced by Asymmetrical Electrode Materials in a Molecular Device. *Appl. Phys. Lett.* **2011**, *98*, 092102.
- (51) Van Dyck, C.; Ratner, M. A. Molecular Rectifiers: A New Design Based on Asymmetric Anchoring Moieties. *Nano Lett.* **2015**, *15*, 1577–1584.
- (52) Van Dyck, C.; Geskin, V.; Cornil, J. Fermi Level Pinning and Orbital Polarization Effects in Molecular Junctions: The Role of Metal Induced Gap States. *Adv. Funct. Mater.* **2014**, 24, 6154–6165.
- (53) Van Dyck, C.; Ratner, M. A. Molecular Junctions: Control of the Energy Gap Achieved by a Pinning Effect. *J. Phys. Chem. C* **2017**, *121*, 3013–3024.
- (54) Lenfant, S.; Guerin, D.; Tran Van, F.; Chevrot, C.; Palacin, S.; Bourgoin, J. P.; Bouloussa, O.; Rondelez, F.; Vuillaume, D. Electron Transport through Rectifying Self-Assembled Monolayer Diodes on Silicon: Fermi-Level Pinning at the Molecule–Metal Interface. *J. Phys. Chem. B* 2006, 110, 13947–13958.
- (55) Smith, C. E.; Xie, Z.; Bâldea, I.; Frisbie, C. D. Work Function and Temperature Dependence

- of Electron Tunneling through an N-Type Perylene Diimide Molecular Junction with Isocyanide Surface Linkers. *Nanoscale* **2018**, *10*, 964–975.
- (56) Broadnax, A. D.; Lamport, Z. A.; Scharmann, B.; Jurchescu, O. D.; Welker, M. E. Ferrocenealkylsilane Molecular Rectifiers. *J. Organomet. Chem.* **2018**, *856*, 23–26.

**Table of Contents artwork** 

